

# Low-cost fiber collimation for MOEMS switches by ink-jet printing

W. Royall Cox,\* Ting Chen, Donald J. Hayes and Michael E. Grove  
MicroFab Technologies, Inc.

## ABSTRACT

Micro-optoelectronic mechanical systems (MOEMS) typically rely on free-space optical interconnects for fiber array in/out connections. The fiber output collimating and input focusing functions may be performed by using either individual gradient-index-of-refraction (GRIN) microlens rods or, more typically, arrays of microlenses formed on a glass substrate, to which the fibers are butte-coupled. We present methods for fabricating, with micron precision, various configurations of micro-optics for fiber collimation using low-cost, ink-jet printing technology. These configurations range from micro-deposition of droplets of optical epoxy into the tips of fibers, positioned in either individual collets or fiber ribbon connector ferrules, to the printing of arrays of collimating/focusing microlenses onto glass substrates. In the latter case the flexibility of the data-driven printing process enables unique capabilities, such as the variation of microlens geometries within an array, in order, for example, to compensate for the varying distances between the input fibers and the individual micro-mirrors within an array of a MOEMS device. The processes and optical modeling approaches used for fabricating such fiber collimation structures utilizing ink-jet printing technology will be discussed in detail, along with process control issues and optical performance data.

**Keywords:** MEMS, MOEMS, microdispensing, ink-jet, micro-optics, fiber collimation

## 1. INTRODUCTION

In the race to develop and bring to the telecom market MOEMS-based optical switches<sup>1</sup>, cost reductions will become increasingly important in determining which products will ultimately prevail. Such devices utilizing micro-mirror arrays rely on free-space optical interconnects typically consisting of 1D or 2D arrays of single-mode optical fibers, with collimating microlenses requiring extremely tight alignment tolerances.<sup>2</sup> As the number of switch ports are increased, these tolerances will become even tighter, thereby, driving up the cost of manufacture of the optical interconnect pieces of the devices. To address this issue we are developing a low-cost, ink-jet printing method of fabricating collimating microlenses directly onto single-mode optical fibers. By this method no lithography is required, because surface tension is used to achieve lens-fiber alignment accuracy, and individual-fiber or fiber-ribbon collimating modules may be readily assembled into one and two dimensional arrays. The high degree of automation and potentially rapid throughput rates ( $\approx 2$  fibers/sec) make this approach especially attractive.

The general advantages of using ink-jet technology for microdispensing derive from the incorporation of data-driven, non-contact processes which enable precise, picoliter-level volumes of material to be deposited with high accuracy and speed at target sites, even on non-planar surfaces.<sup>3</sup> Being data-driven, microjet printing is a highly flexible and automated process which may readily be incorporated into manufacturing lines. It does not require application-specific tooling such as photomasks or screens, and, as an additive process with no chemical waste, it is environmentally friendly. In short, the advantages obtainable with incorporation of micro-jet printing technology in many micro-fabrication applications range from increased process capability, integration and automation, to reduced manufacturing costs.

After a brief overview of ink-jet printing technology we will discuss its application to the printing of microlenses and microlens arrays for optical fiber collimation. The approaches and processes developed for fabricating various component configurations will be detailed, and optical performance data will be presented.

---

\*[rcox@microfab.com](mailto:rcox@microfab.com); MicroFab Technologies, Inc., 1104 Summit Ave., Suite 110, Plano, TX;  
phone: 972-578-8076; fax: 972-423-2438; <http://www.microfab.com>

## 2. INK-JET PRINTING TECHNOLOGY BACKGROUND

### 2.1 Printing Methods

The phenomena of uniform drop formation from a stream of liquid issuing from an orifice were described mathematically by Lord Rayleigh<sup>4</sup> during 1878-1892. Weber<sup>5</sup> used a similar approach as Rayleigh, but produced a much more useful result by making several simplifying assumptions. In the type of system that is based on their observations, shown schematically in Figure 1, fluid under pressure issues from an orifice, typically 50 to 80 $\mu\text{m}$  in diameter, and breaks up into uniform drops by the amplification of capillary waves induced onto the jet, usually by an electromechanical device that causes pressure oscillations to propagate through the fluid. The drops break off from the jet in the presence of an electrostatic field, referred to as the charging field, and thus acquire an electrostatic charge. The charged drops are directed to their desired location, either the catcher or one of several locations on the substrate, by another electrostatic field, the deflection field. This type of system is generally referred to as "continuous" because drops are continuously produced and their trajectories are varied by the amount of charge applied. Theoretical and experimental analysis of continuous type devices, particularly the process of disturbance growth on the jet that leads to drop formation, has been fairly extensive.<sup>6,7</sup> Figure 2 shows a photomicrograph of a 50  $\mu\text{m}$  diameter jet of water issuing from a MicroFab droplet generator device and breaking up due to Rayleigh instability (continuous mode) into 100 $\mu\text{m}$  diameter droplets at 20,000 per second. Continuous mode ink-jet printing systems produce droplets that are approximately twice the orifice diameter of the droplet generator.

In the 1950's, the production of drops by electro-induced pressure waves in fluid under ambient pressure was observed by Hansell.<sup>8</sup> In this type of system, a volumetric change in the fluid is induced by the application of a voltage pulse to a piezoelectric transducer which is directly or indirectly coupled to the fluid. This volumetric change causes pressure/velocity transients to occur in the fluid and these are directed to produce a drop that issues from an orifice.<sup>9,10</sup> Since the voltage is applied only when a drop is desired, these types of systems are referred to as "drop-on-demand." In many commercially available ink-jet printing systems, a thin film resistor is substituted for the piezoelectric drive transducer. When a high current is passed through this resistor, the ink in contact with it is vaporized, forming a vapor bubble over the resistor.<sup>11</sup> This vapor bubble serves the same functional purpose as the piezoelectric transducer. Figure 3 shows a schematic of a drop-on-demand type ink-jet system, and Figure 4 shows a MicroFab drop-on-demand type ink-jet device generating 50 $\mu\text{m}$  diameter drops of ethylene glycol from a device with a 50 $\mu\text{m}$  orifice at 2,000 per second. Demand mode ink-jet printing systems produce droplets that are approximately equal to the orifice diameter of the droplet generator.<sup>12</sup>

### Continuous Mode Ink-Jet Technology

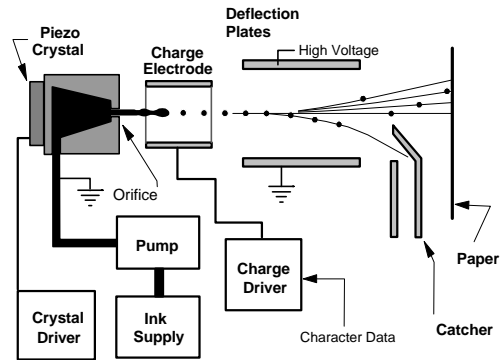


Figure 1. Schematic of a continuous type ink-jet printing system.

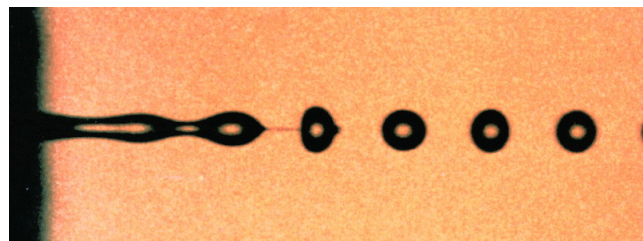


Figure 2. A 50  $\mu\text{m}$  wide jet of water breaking up due to Rayleigh instability into 100 $\mu\text{m}$  droplets at 20 kHz.

### Demand Mode Ink-Jet Technology

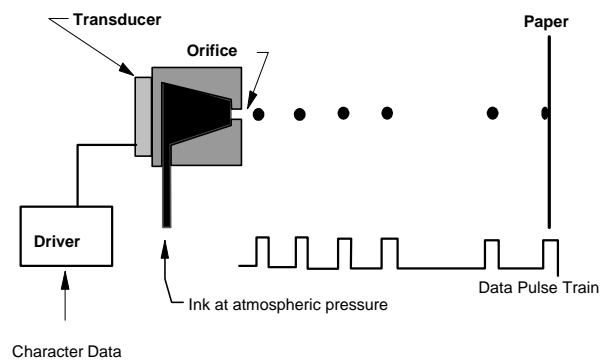


Figure 3. Schematic of a drop-on-demand ink-jet printing system

One of the characteristics of ink-jet printing technology that makes it, in general, attractive as a precision fluid microdispensing technology is the *repeatability* of the process. The images of droplets shown in Figure 2 and Figure 4 were made by illuminating the droplets with an LED that was pulsed at the droplet generation frequency. The exposure time of the camera was  $\sim 1$  second, so that the images represent thousands of events superimposed on each other. The repeatability of the process results in an extremely clear image of the droplets, making it appear to be a high speed photograph. To further illustrate this point, Figure 5 shows two  $60\mu\text{m}$  diameter jets of water that have broken up into  $120\mu\text{m}$  diameter droplets streams at 20,000 per second, and are being caused to merge into a single droplet stream. Again, this image was created using a "strobed" LED and a  $\sim 1$  second exposure time. Not only is the droplet formation process so repeatable that the image of the droplets is sharp, but when the droplets are caused to merge, the formation of the highly contorted merged droplets is seen to be just as repeatable.

Traditionally, drop-on-demand systems have been used primarily in the office printer market, whereas continuous systems are currently in widespread use in the industrial market, principally for product labeling. Continuous mode systems have higher throughput capability and are best suited for high duty cycle applications. They are also more complex than demand mode systems. Although demand mode droplet generation requires the transducer to deliver three or more orders of magnitude greater energy to produce a droplet, compared to continuous mode, which relies on a natural instability to amplify an initial disturbance, piezoelectric demand mode technology is generally more readily adapted to precision fluid microdispensing applications. Unlike continuous mode, demand mode (both piezoelectric and thermal) printing does not require recirculation or wastage of the working fluids. The droplets generated by demand mode devices may be varied in diameter over a wide range, e.g., from  $20\mu\text{m}$  to  $120\mu\text{m}$ , by changing dispensing device orifice diameter and drive waveform. Piezoelectric demand mode does not create thermal stress on the fluid, which decreases the life of both the printhead and fluid. Finally, piezoelectric demand mode does not depend on the thermal properties of the fluid to impart acoustic energy to the working fluid, enabling the dispensing of fluids ranging from polymer formulations to liquid solders.

## 2.2 Piezoelectric Printing Devices

Ink-jet printing devices are either of the single-channel or multiple-channel configuration. For single channel devices, an annular piezoelectric transducer is typically attached to a glass tube with an integrated orifice, as illustrated in Figure 6. Since glass is the only wetted material, this configuration can be used to dispense almost any material with acceptable fluid properties ( $<40\text{cp}$  Newtonian viscosity). Figure 7 shows an example of a single channel printing device with face-seal type of fluid connection, which was designed for high tempera-

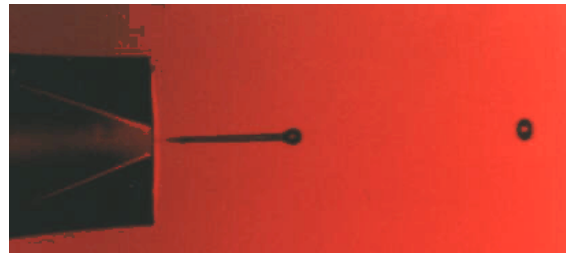


**Figure 4:** Drop-on-demand type ink-jet device generating  $60\mu\text{m}$  diameter drops at  $4\text{kHz}$ .

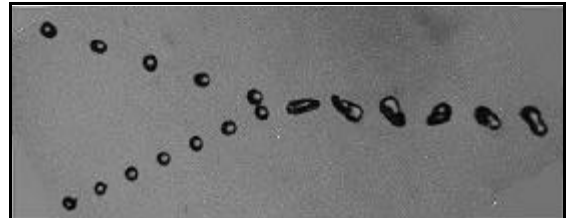


**Figure 5.** Merging of two streams of droplets generated by two drop-on demand printing devices (off left side of photo) operating in phase and at  $2,000\text{ Hz}$ .

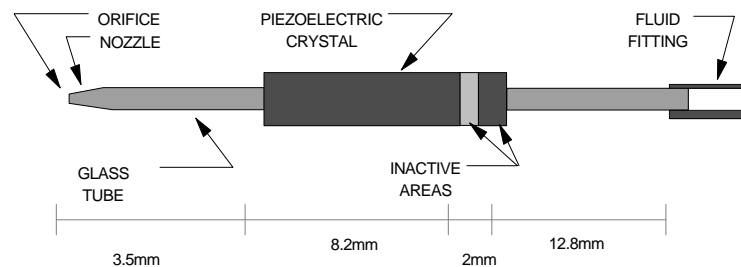


**Figure 6.** Single channel drop-on-demand dispensing device configuration.



**Figure 7.** Single channel,  $33\text{mm}$  long, drop-on-demand device for dispensing at temperatures to  $240^\circ\text{C}$ .

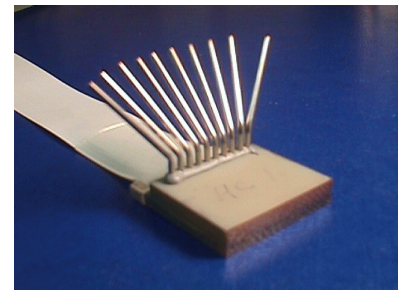


**Figure 8:** 10 channel / 10 fluid integrated array ink-jet printhead, 1 inch wide.

ture operation, mainly through the selection of piezoelectric and adhesive materials, and which can operate continuously at up to 240°C. A multiple channel printing device can be fabricated either by ganging together single channel devices or by utilizing an integrated array<sup>13</sup> printing device, such as the ten-fluid device pictured in Figure 8.

### 3. MICROLENS PRINTING METHODS

High temperature printing devices are utilized for the ink-jet printing of micro-optical elements, in order to enable the microdispensing of 100%-solids formulations of optical prepolymers. The rheology of the optical material determines the temperature required for dispensing, as its viscosity must typically be reduced below 40 cps to enable drop-on-demand ink-jet printing. Droplets may be dispensed in either step-and-print or print-on-fly modes, depending on the lenslet geometries and layout within an array, and at frequencies up to 10,000 drops/sec. Microlens volumes, which are determined by the size and number of deposited droplets, may be adjusted over a wide range and precisely controlled, since droplet diameter repeatability over time is on the order of 1%.

UV-curing optical epoxies are the preferred class of materials for microlens fabrication, because of their superior thermal and chemical durability, as compared to other optical-grade plastics such as acrylics and photoresists. For example, no measurable change in focal length at room temperature has been seen for fully cured optical epoxy microlenses after either exposure to thermal cycles at temperatures as high as 200°C, or thermal aging for hundreds of hours at 85°C. Similarly, no changes in focal lengths of such lenslets, within our measurement resolution of 1-2%, were seen for lenslets measured at elevated temperatures up to 100°C. Until recently, however, a key process challenge in utilizing this type of optical material, as opposed to the less durable thermoplastics which freeze upon impact, has been controlling and arresting the flow of deposited fluid on the substrate until the lenslets may be subsequently solidified by UV-curing. The dispersion curve for our most widely used printable optical epoxies is given in Figure 9.

Recent process advances have overcome the challenge of controlling the flow of uncured material on target substrates and have provided a powerful capability for both varying over a wide range and fine tuning printed microlens aspect ratios within arrays at fixed diameters. This capability is exemplified in the photograph of Figure 10 illustrating the building of microlenses height (or sag) at fixed diameter by adding additional drops of optical material, which, in turn, reduces focal length in accordance with the resulting reduction in lenslet radius of curvature. The range and resolution in focal length adjustment afforded by this process is illustrated by the data of Figure 11. Since the process of building microlens aspect ratio is digital, the resolution available in achieving a target focal length in a microlens of a given diameter increases with the number of deposited droplets, e.g., from 1/400 to 1/1600 along the X-axis in this case. The minimum microlens heights, and hence the longest focal lengths, which may be achieved by this process are determined by differing sets of conditions for smaller and larger diameter lenslets. If the target microlens diameter is not much larger than that of the deposited drop, the minimum lenslet height is limited by the minimum size of one deposited drop. However, when the lenslet diameter greatly exceeds that of the drop diameter, the minimum height is limited by the smallest volume of material which can be made to flow sufficiently to achieve this diameter, which, in turn depends on the wettability of the substrate surface to the deposited material within the target diameter area. On the other hand, the maximum height which can be built in a

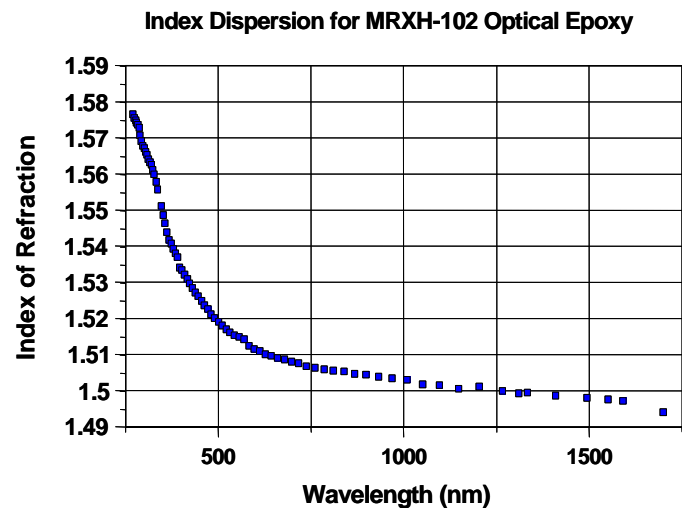


Figure 9: Variation of index of refraction with wavelength for a MicroFab optical epoxy. (Data courtesy of Allen Cox of Honeywell.)



Figure 10. Profiles of 700 μm diameter microlenses printed with (left-to-right) 900, 1400, 1900 & 2400 each 43 μm diameter droplets of optical epoxy.

microlens of any diameter is limited by the surface tension of the printed material relative to the wettability of the surrounding surface. When this limit is exceeded, the additional material is accommodated by an expansion also of microlens diameter rather than purely of height. For a 700  $\mu\text{m}$  diameter microlens the minimum and maximum numbers of 43 $\mu\text{m}$  drops which may be used in printing the lens are about 500 and 2,700, respectively, providing over a factor-of-five in focal length variation by this method. In this case it can be seen that focal length resolution varies over this range, in principle, from about 1.8 to 0.1  $\mu\text{m}/\text{drop}$ .

#### 4. OPTICAL FIBER COLLIMATOR FABRICATION BY INK-JET PRINTING

##### 4.1 Fiber Collimator Modeling

Whenever a plano-convex lens, as apposed to an RGRIN lens rod having a Radial Gradient INdex of refraction,<sup>14</sup> is used for a collimating a light source such as an optical fiber or diode laser, the lens must be physically offset from the light source and be of those dimensions which will, to first order, both put its back focal length at the source plane and contain the diverging source beam within its focal cone, as illustrated schematically in Figure 12. Primary fixed parameters entering into the ray-trace modeling of such systems are, therefore: (a) source divergence angle or numerical aperture, NA; (b) refractive index of the lens and that of any substrate in the optical path at the wavelength of interest; and (c) lens diameter. Other modeling considerations for gaussian beams include second-order adjustments in these parameters for achievement of targets for beam waist diameter and working distance. The results of the modeling exercise which are applicable to collimator fabrication are the variation of collimating lenslet height with offset distance. This is exemplified in Figure 13 for a fiber collimating system consisting of a single mode fiber with NA=0.11 (full cone angle of 12.6°) and a microlens of diameter 1.8 mm with a lenslet index of refraction of 1.5094 at 633 nm, where the offsetting substrate and printed microlens are made from the same optical material.

##### 4.2 Individual Fiber Collimation

The simplest approach for fabricating by ink-jet printing a collimator on the end of a single, free-standing optical fiber is illustrated schematically in Figure 14.<sup>15</sup> The method consists of inserting the fiber tip into a glass tube having inside and outside diameters matching those of the fiber

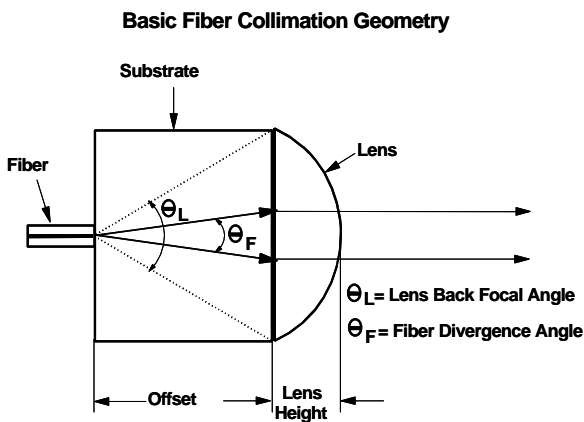


Figure 12: Schematic showing basic geometry for optical fiber collimation by a microlens.

Focal Length vs. Number of Printed Drops (700 micron lenses, 43 micron droplets)

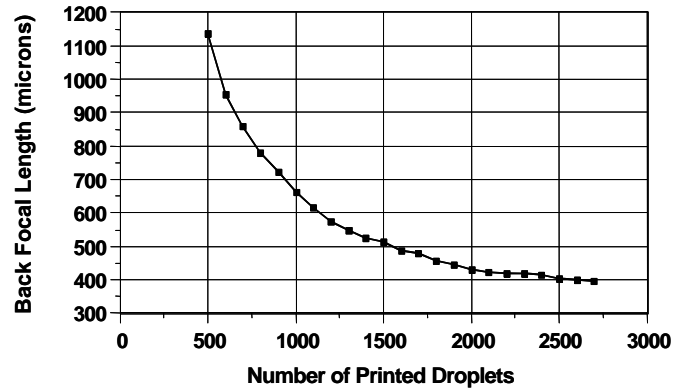


Figure 11: Data illustrating 5x range in printed microlens focal length that can be achieved at a diameter of 700 $\mu\text{m}$ .

Collimating Lens Height vs. Fiber Tip Offset (1.8mm diameter lens; HeNe SM fiber)

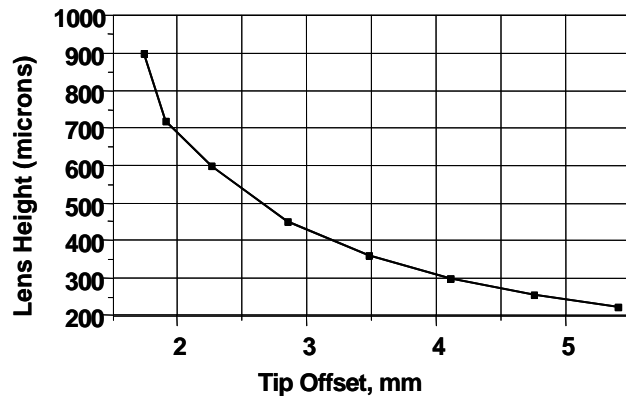


Figure 13: Modeled variation in height of 1.8mm diameter printed microlenses with lens offset from fiber tip, as required for collimation of HeNe wavelength.

and the target microlens, respectively. The offset distance between the fiber tip and the output end of the tube may then be adjusted under a microscope to a target value within  $\pm 2 \mu\text{m}$ , using a fixture to enable fine adjustment of fiber position relative to the tube, prior to securing the fiber in position by applying epoxy to the back end of the tube.

After assembly, the fiber-tube component is then mounted, with open tube end up, onto a printing station chuck under the print head. Two vision systems are required for the optical material printing, a vertical camera for verifying print head location over the fiber and a horizontal one to enable monitoring of the process of filling the tube and measuring the height of the microlens as it is formed on top. Droplets of UV-curing optical epoxy, typically about  $40 \mu\text{m}$  in diameter, are then dispensed into the tube opening until the tube is filled, and a plano-convex microlens of the designed height is formed on top. The outer edge of the tube forms a physical boundary which contains deposited material and allows the lenslet height to be adjusted to any target value within the resolution of the process and up to a maximum value, above which material will overflow the edge of the tube. Maximum lenslet heights achieved to date are on the order of half the diameter, and the resolution in height building is, again, determined by the lens/drop volume ratio. To facilitate filling of the tube without leaving any optically scattering air bubbles, its end may be counter-bored with a taper, as was done in the printed fiber collimator pictured in Figure 15.

After printing the microlens on the end of the glass tube, the entire component is exposed to UV-irradiation in a flood-curing chamber ( $30\text{mW}/\text{cm}^2$  for 45 min.) and then, baked at  $100^\circ\text{C}$  for several hours to achieve a complete cure of the optical epoxy, both within and outside of the tube. During this process a volumetric shrinkage of the optical epoxy, on the order of 1.5%, occurs because of densification, so this must be taken into account when adjusting lenslet height during printing.

Beam collimation performances of our printed microlens collimators are currently measured using a HeNe laser as a source and a beam analyzer with silicon detector. Data collected by this system include beam spot size as a function of distance from the fiber tip or collimating lenslet, as well as beam circularity and directionality relative to the optical axis. Typical data comparing beam divergence between a single mode optical fiber with and without a printed microlens collimator are given in Figure 16. In this example, application of the microlens produced about a four-fold reduction in beam numerical aperture.

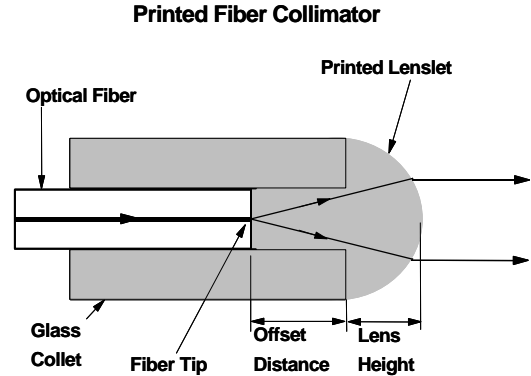


Figure 14. Schematic illustration of forming a collimating microlens on the tip of an optical fiber by ink-jet printing.

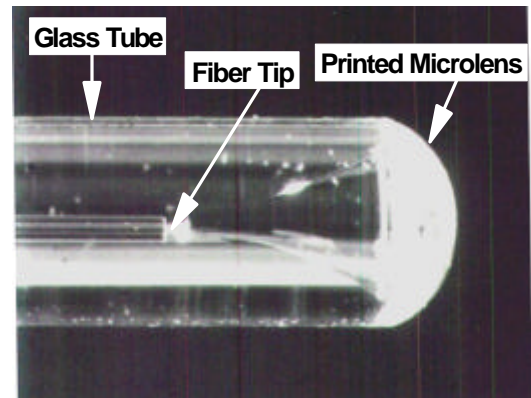


Figure 15. Fiber collimator fabricated by printing  $43 \mu\text{m}$  drops of optical epoxy to form a lens on end of glass tube, into which fiber has been inserted (magnification = 20X).

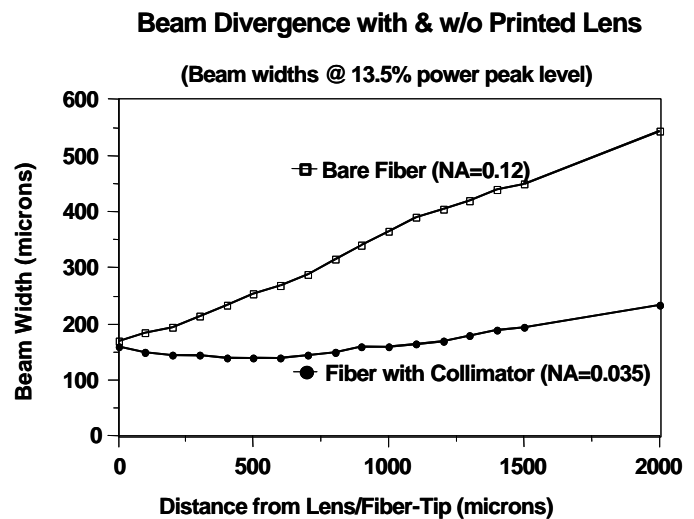


Figure 16. Comparison of beam divergence angle of a single-mode fiber with and without printed microlens collimator.

### 4.3 Fiber Array Collimation

Collimation of arrays of optical fibers by ink-jet printing may be accomplished by several differing methods. A modular approach may be employed, whereby individual fibers with collimating lenslets printed onto glass tubes (as in Figure 15) may be ganged together to form 1D or 2D arrays, by inserting the tubes into a manifold having holes on the requisite centers and with diameters matching that of the tubes. Alternatively, an array of collimating microlenses may be printed onto a glass substrate at the fiber center-to-center distance, with the lenslet geometry and substrate thickness adjusted to put the microlens back focal length at or near the back side of the substrate, according to design criteria. Then the microlens array is aligned with a manifold supporting a corresponding array of optical fibers and epoxied to the backside of the microlens substrate. The photograph of Figure 17 is an example of an array of microlenses printed for use in fiber array collimation. Here an array of 916 $\mu$ m diameter microlenses was printed on 1 mm centers onto a 1mm thick, treated glass substrate, and the number of 40 $\mu$ m diameter droplets was adjusted to put the back focal length of the lenses at the back of the substrate. Microlens relative placement errors on the substrate are at the submicron level. Similarly, as illustrated by the diameter distribution data of Figure 18, standard variations among lenslet diameters are on the order of 0.02%. With uniform curing of printed material and very tight control of both microlens diameters and volumes, focal lengths within a printed array may be controlled to better than the 1% resolution of the measurement method, as indicated by the focal length distribution data of Figure 19.

Another approach for fabricating arrays of collimating fibers by ink-jet printing is to insert the fibers part way through the holes of a manifold and print optical material into the holes on top of the fiber tips until plano-convex microlenses are formed on the top surface of the manifold, similar to the method described for individual fiber collimation. The simplest demonstration of this is the fabrication of a 1 x n array fiber ribbon collimator. Here a standard fiber ribbon-connector ferrule may be used as the manifold when fiber centering on 250  $\mu$ m spacings is required. Unlike the individual fiber collimators, however, there is no physical edge, e.g., tube diameter, to arrest the flow of deposited fluid and allow the building of plano-convex lenslets over the fibers. In a ferrule fixture this challenge may be met in a number of ways, such as by micromachining grooves of the lenslet design diameter around each hole. An alternative method we have employed is treating the surface of the ferrule with a chemical coating which is de-wetting to the optical material, thereby inhibiting

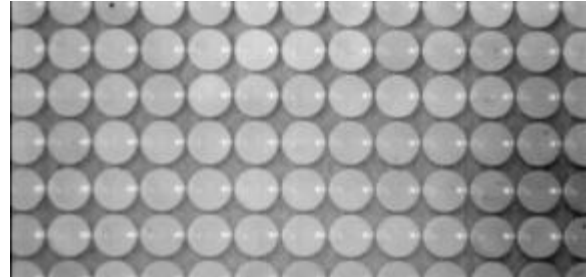


Figure 17. Array of 916  $\mu$ m diameter microlenses printed on 1 mm centers.

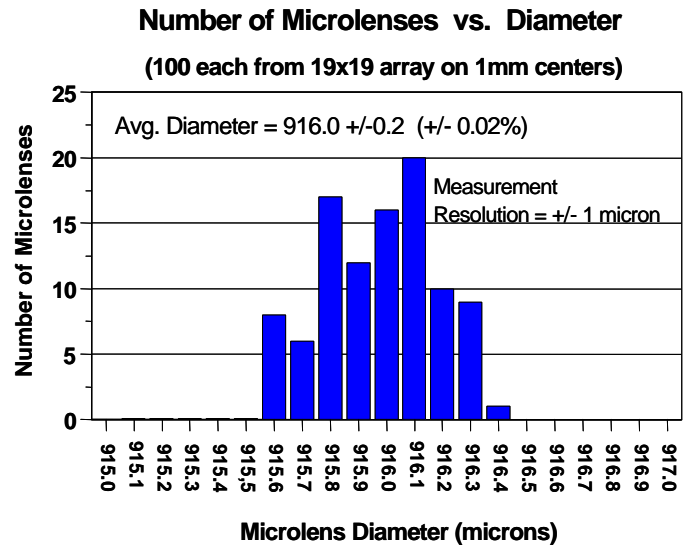


Figure 18: distribution of diameters within the microlens array of Figure 17, showing standard deviation of 0.2 $\mu$ m.

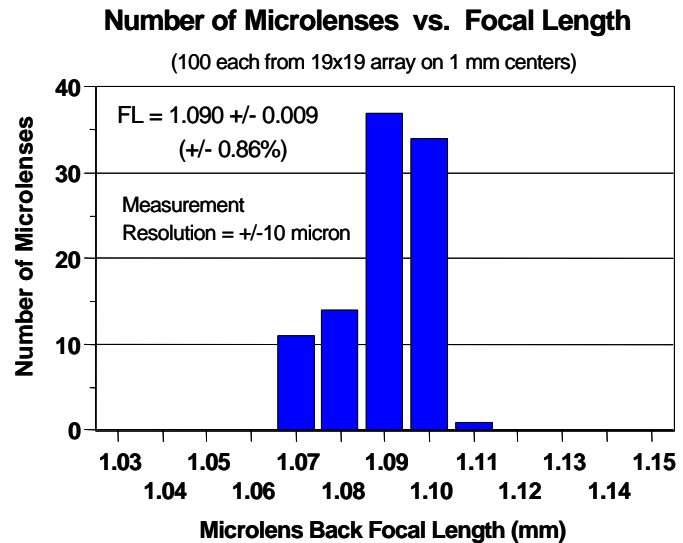
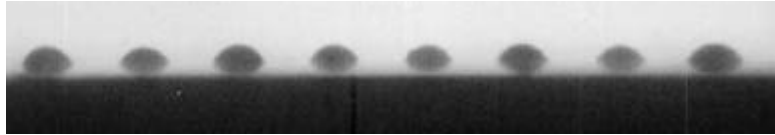


Figure 19. Distribution of back focal lengths (through substrate) within the microlens array of Fig. 17, showing standard deviation of less than 1%.

material flow away from the 126  $\mu\text{m}$  diameter fiber holes. The procedure for locating the fibers of the ribbon in the ferrule holes at the design offset distance, then microdepositing droplets of optical epoxy in each one to achieve the corresponding lenslet height, is essentially the same as for individual fiber collimation. An example of fiber ribbon collimator fabricated in this way is pictured in Figure 20.



**Figure 20.** 1 x 8 array of fiber collimators for fiber ribbon applications, showing 126 $\mu\text{m}$  diameter microlenses printed on 250 $\mu\text{m}$  centers on top of a connector ferrule.

## 5. SUMMARY AND CONCLUSIONS

We have shown how the ink-jet printing method may be employed to fabricate low-cost collimators for optical fibers, both individually and within arrays. The different approaches included: (a) printing microlenses onto the ends of glass tube collets for individual fiber collimation; (b) printing microlenses onto fiber ribbon connector ferrules for ribbon collimation applications; and (c) printing of arrays of collimating microlenses onto glass substrates for 2D fiber array collimation. For the latter approach we have presented data showing how process advances in micro-optics printing technology have enabled a new capability for varying the heights/sags of microlenses of a fixed diameter over wide ranges and with very high resolution. The relative locations and diameters of printed microlenses within such arrays can be controlled to sub-micron and micron accuracies, respectively. In short, this new micro-optics printing process combines lithographic-level placement and planar-dimensional accuracies with the capability for printing microlenses with profiles varying from nearly flat to hemispherical. Thus, micro-optics printing technology is now able to provide both superior flexibility and competitive fabrication precision, compared to alternative technologies, while retaining its previously established advantages of low-cost, high level of process automation and integration, and environmental friendliness.

For microlenses with diameters in the 600-900  $\mu\text{m}$  range often utilized in MOEMS assembly for collimation and focusing of beams into and out of the devices, respectively, we have shown that focal lengths may be finely adjusted and tightly controlled within the arrays to the degrees required of this demanding application. The data-driven nature of this technology also provides a unique capability which could be utilized to advantage in fabricating microlens arrays for use in MOEMS devices, namely, the fine-tuning of microlens focal lengths within the same array, in order to compensate for the relatively large and varying fiber-to-micro-mirror distances.

Ongoing and near-future work include the fabrication of precision arrays of microlens for incorporation into a 6x6 MOEMS switch, development of processes for printing microlenses for increasing the efficiency of coupling of VCSEL arrays to fiber ribbons, and the fabrication of microlens arrays for various imaging applications.

## ACKNOWLEDGMENTS

The underlying foundations and various components of this work have been supported in part by DARPA, via: the U.S. Army Research Office in Triangle Park, NC; the U.S. Army Aviation and Missile Defense Command in Redstone Arsenal, AL; and the Honeywell Technology Center in Minneapolis, MN. Initial funding for developing this technology were from the U.S. Air Force Phillips Lab in Albuquerque, NM. Additional contributors within MicroFab include Hans-Jochen Trost and Rick Hoenigman. To all we express thanks.

## REFERENCES

1. K. Lewotsky, "MEMS pack a technology punch," *SPIE OE Magazine*, pp.22-29, May, 2001.
2. E. Kruglick, "MEMS crossconnects demand precision from design to delivery," *WDM Solutions Magazine*, pp.103-105, March, 2001.
3. W.R. Cox, T. Chen and D.J. Hayes, "Micro-optics fabrication by ink-jet printing," *OSA Optics & Photonics News*, pp.32-35, June, 2001.

4. Lord Rayleigh, "On the instability of jets," *Proc. London Math Soc.* **10**, No. 4 (1878).
5. Weber, C., "Zum zerfall eines flussigkeitsstrahles," *Z. Angew. Math. Mech.* **11**, no.136, 1931.
6. Chaudhary, K.C., I.G. Redekopp, and T. Maxworthy, "The non-linear capillary instability of a liquid jet," *Journ. Fluid Mech.* **96**, part II, pp. 257-312, 1979.
7. Pimbley, W.T., "Drop formation from a liquid jet: a linear one-dimensional analysis considered as boundary value problem," *IBM Journ. Res. Dev.* **29**, pp. 148-156, 1984.
8. Hansell, U.S. Patent 2,512,743, 1950.
9. Bogy, D.B. and F.E. Talke, "Experimental and theoretical study of wave propagation phenomena in drop-on-demand ink jet devices," *IBM Journ. Res. Develop.* **29**, pp. 314-321, 1984.
10. Dijkstra, J.F., "Hydrodynamics of small tubular pumps," *Journ. Fluid Mech.* **139**, pp. 173-191, 1984.
11. J.S. Aden, J.H. Bohorquez, D.M. Collins, M.D. Crook, A. Garcia, and U.E. Hess, "The third generation thermal inkjet printhead," *Hewlett-Packard Journal* **45**, 1, pp. 41-45, 1994.
12. Wallace, D.B., "A method of characteristics model of a drop-on-demand ink-jet device using an integral method drop formation model," ASME publication **89-WA/FE-4**, December 1989.
13. D.B. Wallace, V. Shah, D.J. Hayes, and M.E. Grove "Photo-realistic ink jet printing through dynamic spot size control," *J. of Imaging Sci. & Tech.* **40**, pp. 390-395, 1996.
14. D.T. Moore, "Gradient-index optics: a review," *Applied Optics* **19**, No. 7, pp. 1035-1038, 1980.
15. W.R. Cox, C. Guan and D.J. Hayes, "Microjet printing of micro-optical interconnects and sensors," *Photonics West Proceedings*, **3952**, pp. 400-407, 2000.